Ultrastructural findings in feline corneal sequestra

Cheryl L. Cullen,* Dorota W. Wadowska,† Amreek Singh‡ and Yuri Melekhovets§

Department of Companion Animals, †Graduate Studies and Research, and ‡Department of Biomedical Sciences, Atlantic Veterinary College, University of Prince Edward Island, 550 University Avenue, Charlottetown, Prince Edward Island, Canada C1A 4P3; §HealthGene Corporation, Molecular Diagnostic and Research Center, 2175 Keele Street, Toronto, Ontario, Canada M6M 3Z4

Address communications to:

Cheryl L. Cullen

Tel.: (902) 566–0950
Fax: (902) 628–4316
e-mail: clcullen@upei.ca

Abstract

Objectives (1) To describe the ultrastructural features of corneal sequestra in cats; and (2) to enhance our understanding regarding the pathogenesis of feline corneal sequestration. *Methods* Nine corneal sequestra were harvested via keratectomy from globes of nine cats. The sequestra were routinely fixed then postfixed for high resolution light and transmission electron microscopy (HR-LM and TEM, respectively). The tissues were embedded in Epon/Araldite. Sections of 0.5-μm thickness were cut and stained with 1% toluidine blue in 1% sodium tetraborate solution for HR-LM. Ultrathin sections were collected on copper grids and stained with uranyl acetate and Sato's lead stain for TEM. Ultrathin sections were examined and the images were captured on an Advantage HR CCD camera using a Hitachi 7500 electron microscope operated at 80 kV. Two healthy corneas from two cats were harvested immediately following euthanasia. These corneal tissues (control samples) were processed in the same manner as the corneal sequestra for HR-LM and TEM. A portion of each sequestrum was also submitted for polymerase chain reaction (PCR) testing for infectious agents including feline herpesvirus-1 (FHV-1), *Toxoplasma gondii*, *Chlamydophila felis* and *Mycoplasma* spp.
Results Ultrastructure of healthy corneal tissues revealed basal corneal epithelial cells aligned adjacent to a thin acellular layer similar to Bowman's layer with underlying tightly packed, regularly arranged, collagen fibrils oriented in different planes. Keratocytes were elongated and had long and irregularly shaped nuclei, and cytoplasm contained rough endoplasmic reticulum and abundant membrane-bound vesicles. In contrast, corneal sequestra contained varying amounts of an amorphous, electron-dense substance, continuous with intact basal epithelial basement membranes peripherally, and overlying corneal ulceration and loosely packed collagen fibrils. Remnants of necrotic keratocytes were seen in spaces between disarranged collagen layers. In all samples, occasional keratocytes exhibited morphology indicative of apoptosis including clumping and margination of chromatin, and shrunken cytoplasm. Varying degrees of inflammation were noted on HR-LM and TEM of affected corneas including peri- and intralesional neutrophils, lymphocytes, plasma cells, and macrophages. Corneal sequestra were FHV-1-positive (*n* = 3), FHV-1- and *T. gondii*-positive (*n* = 1), *T. gondii*-positive (*n* = 3), or negative for DNA of these infectious agents (*n* = 2) using PCR. All corneal sequestra were negative for DNA of *Chlamydophila felis* and *Mycoplasma* spp. using PCR.
Conclusions Apoptosis may play a role in the pathogenesis of feline corneal sequestration independent of the presence of DNA of these infectious organisms. Prospective clinical studies are warranted to further understand the significance of *T. gondii* in relation to feline corneal sequestration.

Key Words: corneal nigrum, corneal sequestrum, polymerase chain reaction, transmission electron microscopy

INTRODUCTION

Corneal sequestration has been documented in cats and horses.[1-6] The classic clinical manifestation of feline corneal sequestra includes central to paracentral corneal discoloration ranging from a faint transparent tea-color to an opaque black pigmentation. Varying degrees of corneal vascularization with or without overlying corneal ulceration may also accompany the corneal sequestrum. In certain cases, mineralization of the necrotic corneal stroma may arise.[2] Although the cause(s) and pathogenesis(es) for this corneal disease in the cat are yet to be completely elucidated, several contributing factors have been described including corneal trauma, chronic ulcerative keratitis, breed predisposition (Persian, Himalayan, Siamese), brachycephalic conformation with lagophthalmos, exposure keratopathy, chronic corneal irritation, topical corticosteroid use, primary corneal dystrophy, altered corneal stromal metabolism, qualitative tear film deficiencies, and feline herpesvirus type-1 (FHV-1) infection.[1-7] A recent study used various laboratory techniques to attempt characterization of the nature of the discoloration in feline corneal sequestration.[8] Scanning electron microscopy revealed the presence of particles within the corneal sequestra that were consistent with the appearance of melanin granules.[8] To our knowledge, one case report documents the transmission electron microscopic findings in a feline corneal sequestrum.[4]

The aims of the present study were: (1) to describe the ultrastructural features of corneal sequestra in cats; and (2) to enhance our understanding regarding the pathogenesis of feline corneal sequestration by reviewing historical, clinical, and laboratory findings obtained from affected cats for which the ultrastructural features of the corneal sequestra were evaluated.

MATERIALS AND METHODS

Medical records of cats diagnosed with corneal sequestration, treated surgically, and having had a portion of necrotic corneal tissue submitted for high resolution light and transmission electron microscopy (HR-LM and TEM) between March 2002 and November 2004 at the Atlantic Veterinary College (AVC) of the University of Prince Edward Island, were reviewed.

Historical, clinical, and laboratory findings
Each cat had undergone a complete ophthalmic examination including neuro-ophthalmic examination, Schirmer tear test (Schirmer tear test strips; Alcon Canada, Mississauga, Ontario, Canada), fluorescein dye staining (Fluor-I-Strip AT; Ayerst Laboratories, St. Laurent, Quebec, Canada), applanation tonometry (Tonopen XL; Biorad Ophthalmic Division, Santa Clara, CA, USA), slit-lamp biomicroscopy (Kowa SL-14; Kowa, Tokyo, Japan) and indirect ophthalmoscopy (Keeler All Pupil Indirect; Keeler Instruments, Inc., Broomall, PA, USA). The corneal sequestration was treated surgically in all cases by performing a keratectomy (with or without placement of a conjunctival pedicle flap or conjunctival island graft) to allow adequate necrotic corneal tissue for further diagnostic testing.

In each case, historical information including signalment, lifestyle (indoor/outdoor), diet, presence or absence of systemic illness, and duration of ocular disease was reviewed. In addition, the presenting physical examination and ophthalmic findings, blood (complete blood count (CBC) and serum biochemical profile) and urinalysis (n = 6/9 cats) test results, and polymerase chain reaction (PCR) results obtained from corneal sequestrum and blood samples were reviewed. Specifically, PCR tests for the following infectious agents had been performed on a portion of corneal sequestrum and blood samples from each cat: feline herpesvirus-1 (FHV-1) and *Toxoplasma gondii* (n = 9/9 cats), and *Chlamydophila felis* and *Mycoplasma* spp. (n = 5/9 cats) (HealthGene Corporation, Molecular Diagnostic Research Center, Toronto, Ontario, Canada). *Toxoplasma gondii* had been included prospectively in the diagnostic screening for all affected cats following the first case from which a portion of the corneal sequestrum had been submitted for HR-LM and TEM. This affected cat was an indoor/outdoor cat with a recent history of diminished appetite. As such, blood and corneal sequestrum from this cat were submitted for PCR testing for *T. gondii* and both samples were positive for this infectious agent.

High resolution light microscopic and ultrastructural studies
A portion of keratectomy specimen from the corneal sequestrum of each cat was fixed in 2% glutaraldehyde in 0.1 M phosphate buffer (pH 7.2) and was submitted for HR-LM and TEM examinations. Following 1 h of glutaraldehyde fixation at 22 °C, blocks approximately 1×3 mm were cut from the corneal sequestra incorporating both the central and peripheral aspects of each corneal sample, for each of the three cats. The tissues were then postfixed at 22 °C in 1% osmium tetroxide in 0.1 M phosphate buffer (pH 7.2) for 1 h, dehydrated in ethanol and propylene oxide, and embedded in Epon/Araldite. Sections 0.5 μm thick were cut and stained with 1% toluidine blue in 1% sodium tetraborate solution for HR-LM. Ultrathin sections were collected on copper grids and stained with uranyl acetate and Sato's lead stain for TEM. Ultrathin sections were examined and the images were captured on a Hamamatsu AMT Advantage HR CCD camera (Hamamatsu Photonics; Hamamatsu City, Shizouka Pref, Japan) using a Hitachi 7500 electron microscope (Hitachi High Technologies Corporation; Tokyo, Japan) operated at 80 kV. Two healthy corneas, one from an approximately 2-year-old Domestic Short-haired cat (DSH) and the other from an approximately 9-year-old DSH cat, were harvested immediately following unrelated euthanasia. These corneal tissues were processed in the same manner as the corneal sequestra and were used as age-matched, control samples for HR-LM and TEM.

RESULTS

Historical, clinical, and laboratory findings

Table 1 details the historical, clinical, and laboratory findings for each cat. Briefly, there were nine cats from which ultrastructural features of the corneal sequestrum were obtained. The affected cats ranged in age from 1.5 to 12 years (mean = 5.7 years). Four of the nine affected cats were Himalayan. The majority of cases were indoor cats only (*n* = 7/9 cats). All cats were fed a commercial cat food. Systemic abnormalities reported by the owners included: weight loss and depression noted a few weeks earlier (*n* = 1 cat); short-term diminished appetite (*n* = 1 cat); and previous upper respiratory signs (*n* = 1 cat). Current systemic abnormalities were not reported by the owners. Physical examinations were unremarkable other than the ocular findings. None of the cats had evidence of ocular disease other than the corneal sequestrum with varying degrees of corneal vascularization (*n* = 8/9 eyes) and edema, and overlying ulceration. There were no remarkable findings on CBC and serum biochemical profile or the urinalysis of any cat.

Four of the nine cats were positive for *T. gondii* DNA in the corneal sequestra with two of these four cats also being positive for *T. gondii* DNA in the blood and the other two cats having positive IgG titers for *T. gondii*. One *T. gondii*-affected cat was also positive for FHV-1 DNA in the corneal and blood samples, and two *T. gondii*-affected cats had FHV-1-positive blood samples. Two corneal samples were positive for FHV-1 DNA only. All samples tested were negative for *Chlamydophila felis* and *Mycoplasma* spp. Summarized in Table 1 are the PCR results. The *T. gondii*-positive cases were treated with oral clindamycin (12.5 mg/kg PO q12 h for 2 weeks or 20 mg/kg PO q12 h for 3 weeks for cases 8, 6 and 1, and case 2 (Table 1), respectively). None of these four cases returned to the AVC for follow-up as no recurrent corneal sequestration was observed by the owners or the referring veterinarians following 1.5, 3.5, 24, and 33.5 months, respectively. Consequently, no additional samples for PCR testing or serology for *T. gondii* were obtained following treatment.

High resolution light microscopic and ultrastructural findings

HR-LM revealed similar findings for all nine corneal sequestra. The samples contained ulcerated surfaces with varying degrees of irregular, mono-layered, loose corneal epithelium extending to, and occasionally partially overlying, the periphery of the dorsal aspect of the sequestered tissue (Fig. 1). Each corneal sequestrum consisted of a large focal area of acellular stromal collagen (corneal stromal necrosis) demarcated peripherally and at its base by leukocytes (primarily neutrophils with some lymphocytes and plasma cells), fibroblasts, and keratocytes (fibrocytes) with occasional inflammatory cells in the lesions (Fig. 1). One animal (case 2; Table 1) had multiple aggregates of cocci-like micro-organisms surrounding and within the collagen suggestive of *Staphylococcus* sp.

Ultrastructure of healthy corneal tissues from both the young and the old DSH cats were similar in appearance. In

Table 1. Historical and clinical findings, and polymerase chain reaction test results for nine cats with corneal sequestration

Case	Breed	Age (years)	Gender†	Systemic signs	Lifestyle	Duration of ocular disease	Corneal vascularization‡	Toxoplasma gondii DNA blood	Toxoplasma gondii DNA cornea	Toxoplasma gondii serologic titers	FHV-1 DNA blood	FHV-1 DNA cornea
1	Himalayan	3	MN	Short-term decreased appetite	Indoor/outdoor	2 months	Y	+	+	NA	+	+
2	Himalayan	1.5	FS	Weight loss and depression a few weeks prior to presentation	Indoor	2 months	Y	+	+	NA	+	–
3	Cornish Rex	7.5	MN	None	Indoor	2.5 months	Y	–	–	NA	+	+
4	Himalayan	8	FS	None	Indoor	4 months	Y	–	–	NA	–	–
5	Siamese	3.5	MN	None	Indoor	1.5 months	Y	–	–	NA	+	+
6	DLH*	8.5	FS	None	Indoor	2.5 months	N	–	+	IgG + (1 : 512)/IgM : NA	+	–
7	Himalayan	12	FS	None	Indoor	2 months	Y	–	–	NA	–	–
8	Abyssinian	4.5	MN	Upper respiratory signs	Indoor/outdoor	3 months	Y	–	+	IgG + (1 : 256)/IgM	–	–
9	DLH	2.5	FS	None	Indoor	4 months	Y	–	–	NA	–	+

*DLH, Domestic Long-hair; †MN, male neutered; FS, female spayed; ‡Y, yes; N, no; FHV-1, feline herpesvirus type-1.

Figure 1. Toluidine blue-stained section of a portion of the corneal sequestrum from case 2 (see Table 1). Note the ulcerated dorsal surface overlying the acellular necrotic stromal collagen and surrounding inflammatory infiltrate; bar scale = 100 μm.
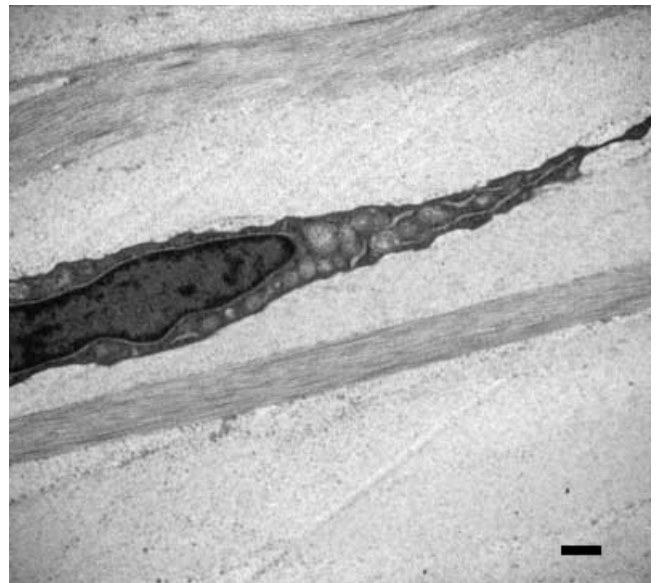

Figure 2. Ultrastructure of healthy cornea from a young Domestic Short-haired cat. Depicted are alignment of basal corneal epithelium along a thin acellular layer (*), keratocytes (K), and collagen layers composed of tightly packed, regularly arranged, interbranching fibrils oriented either longitudinally or tangentially. ×6000; bar scale = 2 μm.

Figure 3. Elongated appearance of a keratocyte, which contains nucleus with marginated chromatin, cytoplasm with abundant membrane-bound vesicles filled with electron lucent material and rough endoplasmic reticulum, is illustrated. ×15 000; bar scale = 500 nm.

Figure 4. Electron micrograph of the anterior-most aspect of the corneal sequestrum from case 1 (see Table 1) to demonstrate corneal ulceration with an amorphous, electron-dense substance in place of normal epithelial cells and overlying irregularly arranged collagen fibrils. ×7000; bar scale = 2 μm.

particular, the basal corneal epithelial cells were aligned adjacent to a thin acellular layer similar to Bowman's layer (Fig. 2). Numerous hemidesmosomal junctions were present between this layer and the overlying epithelial cells. Underlying collagen layers were composed of tightly packed, regularly arranged, interbranching collagen fibrils oriented in different planes (Fig. 2). Keratocytes, positioned between layers of collagen, were elongated and had long and irregularly shaped nuclei (Fig. 2), and cytoplasm containing rough endoplasmic reticulum and abundant membrane-bound vesicles filled with electron lucent material (Fig. 3). In contrast, all of the corneal sequestra, whether positive for FHV-1

and/or *T. gondii* DNA or not, contained varying amounts of an amorphous, electron-dense substance, continuous with intact basal epithelial basement membranes peripherally, and overlying corneal ulceration and loosely packed collagen fibrils (Fig. 4). Remnants of necrotic keratocytes were seen in spaces between disarranged collagen layers illustrated in
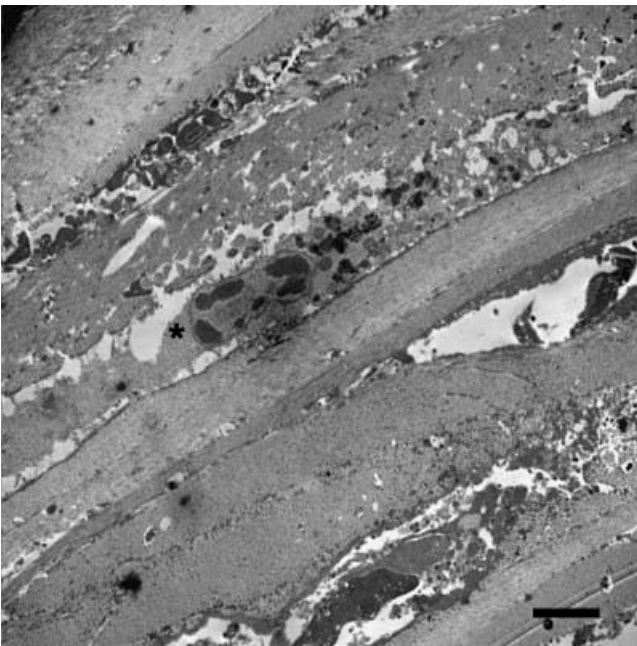
Figure 5. Ultrastructure of the mid-stroma of the corneal sequestrum from case 3 (see Table 1). Note the remnants of necrotic keratocytes located in spaces between disarranged collagen layers, and a keratocyte with nuclear clumping and margination of chromatin (*), and shrunken cytoplasm indicative of apoptosis. ×7000; bar scale = 2 μm.
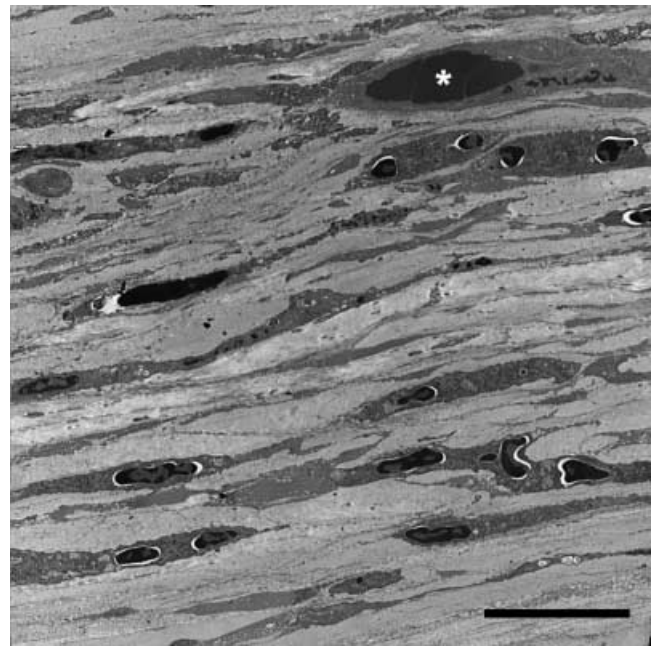

Figure 6. Ultrastructure of the mid-stroma of the corneal sequestrum from case 4 (see Table 1). Note the high surface ratio of keratocytes to collagen, and the vascularization of the corneal stroma as depicted by the presence of a small blood vessel filled with erythrocytes (*). ×3000; bar scale = 10 μm.

Fig. 5. Occasional keratocytes exhibited morphology indicative of apoptosis including clumping and margination of chromatin, and shrunken cytoplasm (Fig. 5). One corneal specimen that was negative for the DNA of infectious agents (case 4; Table 1) had an area of numerous keratocytes or fibrocytes present between tightly packed layers of collagen (Fig. 6). The keratocytes appeared elongated to ovoid to irregular in shape and were often seen clustered in groups of two or more cells positioned between layers of collagen (Fig. 6). This same corneal sample also had corneal epithelial cells that were irregular in shape with electron-dense cytoplasm and well preserved organelles overlying the peripheral sequestered stroma (Fig. 7). Nuclei of the epithelial cells were irregular in shape and contained large granular inclusions (Fig. 7). One corneal sample which was *T. gondii*-negative and FHV-1-positive with PCR (case 3; Table 1) contained circular to irregularly shaped, electron-dense deposits of diverse size scattered over and amidst necrotic collagen fibrils (Fig. 8). The larger deposits showed concentric arrangements of varied electron densities with the outermost layer being the most electron dense (Fig. 8). Smaller deposits were presented as irregular, electron-dense granules. Inflammatory cells, mainly neutrophils and occasional mononuclear cells, were located between bundles of necrotic collagen; some neutrophils contained phagocytized collagen fibrils (Fig. 9) while some macrophages were in the process of phagocytizing remnants of cells (Fig. 10). One corneal sequestrum (case 2; Table 1) had micro-organisms infiltrating the diseased

Figure 7. Ultrastructure of corneal epithelium overlying the peripheral anterior stroma of the corneal sequestrum from case 4 (see Table 1). Note the irregularly shaped corneal epithelial cells with electron-dense cytoplasm, and the irregularly shaped nuclei containing large granular inclusions (arrow). ×6000; bar scale = 2 μm.
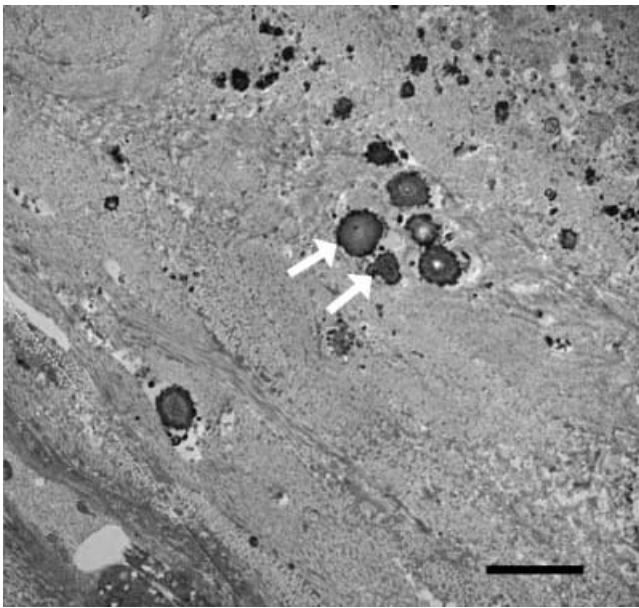
Figure 8. Ultrastructure of the anterior stroma of the corneal sequestrum from case 3 (see Table 1). Note the circular to irregularly shaped, electron-dense deposits of diverse size amidst necrotic collagen fibrils (arrows). The larger deposits exhibit concentric arrangements of varied electron densities with the outermost layer being the most electron dense. ×10 000; bar scale = 2 μm.
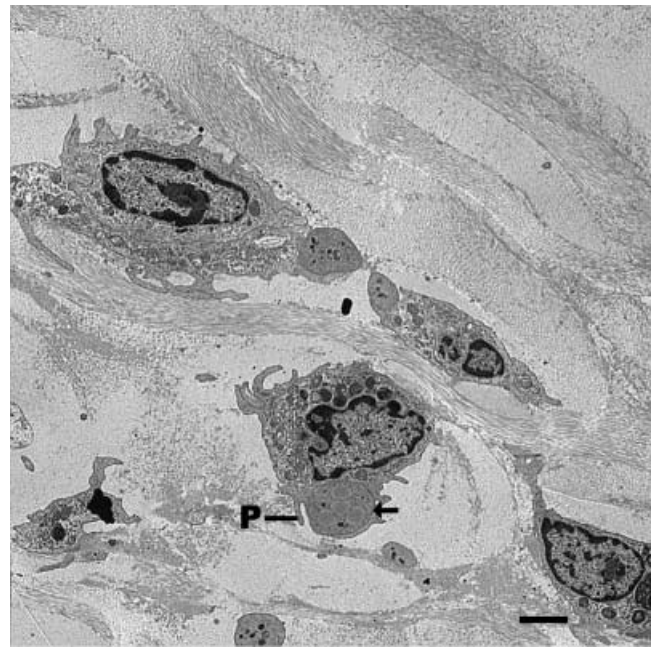

Figure 10. Ultrastructure of a portion of the corneal sequestrum from case 9 (see Table 1) to demonstrate macrophages phagocytizing cellular remnants. Note the remnants of cells that are being engulfed by pseudopods (P) and those which are internalized in the phagocytic vacuole (arrow). ×5000; bar scale = 2 μm.
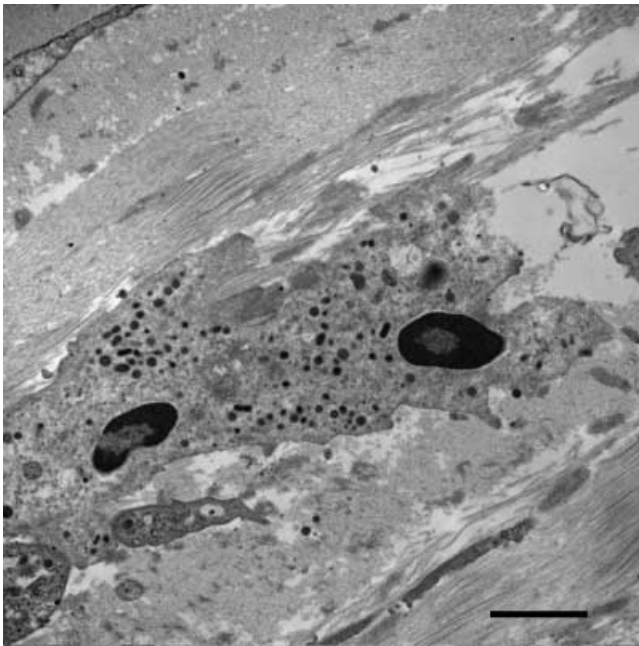

Figure 9. Ultrastructure of a portion of the corneal sequestrum from case 3 (see Table 1) to demonstrate neutrophils phagocytizing collagen fibrils. ×10 000; bar scale = 2 μm.
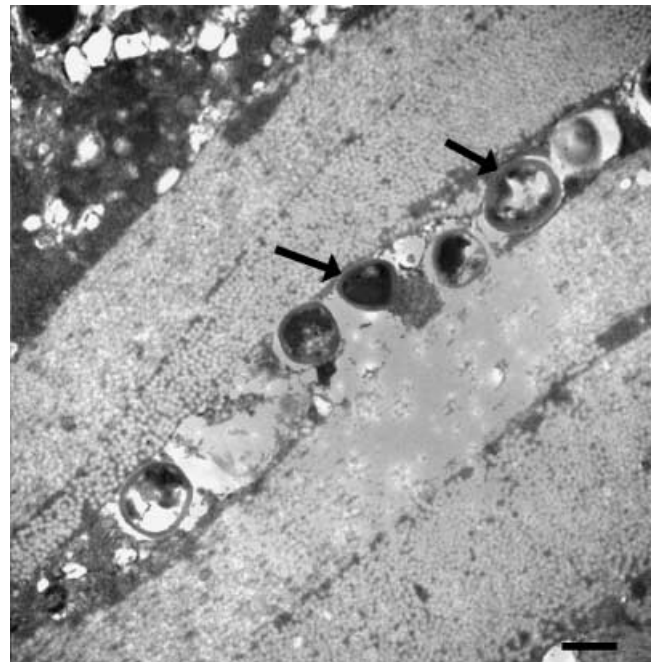

Figure 11. Electron micrograph of micro-organisms infiltrating between collagen layers of the diseased cornea of case 2 (see Table 1). Round to ovoid or triangular organisms with electron lucent cores and dense granulation are depicted (arrows). The morphology and size of these organisms were consistent with *Staphylococcus* sp. ×20 000; bar scale = 500 nm.

cornea between collagen layers (Fig. 11). Organisms displayed different shapes ranging from round to triangular, and possessed a wall thickness from 66 to 88 nm. The triangular core of some of these organisms was electron dense while

that of round and ovoid organisms was electron lucent with dense granulation located peripherally (Fig. 11). The size of these organisms ranged from 500 to 600 nm; morphology and size were consistent with *Staphylococcus* sp.

DISCUSSION

In the current study, the presence of necrotic keratocytes, disarranged collagen, and peri-lesional inflammatory cells detected with TEM in all cases of corneal sequestra is compatible with a previous report documenting the electron microscopic findings in a corneal sequestrum from a Siamese cat.[4] The amorphous, electron-dense substance noted with TEM, continuous with an intact epithelial basement membrane peripherally and overlying irregularly arranged collagen fibrils on the anterior surface of all corneal sequestra, may be compatible, in part, with degraded epithelial basement membrane. Animal models of corneal ulceration demonstrate that the basement membrane is degraded actively by products of corneal cells.[9] In a thermal model of corneal ulceration, as new matrix is being deposited in the burned tissue, matrix metalloproteinase 2 (MMP-2) appears in the cornea.[9] The timing of expression of MMP-2 suggests a role for this enzyme in appropriate deposition and remodeling of new matrix in the regenerating corneal tissue. The exaggerated, degraded epithelial basement membrane noted ultrastructurally in all nine cases of corneal sequestration may be the result of inappropriate gelatinase activity from corneal cells. Further studies would be required to investigate this possibility.

TEM of the necrotic corneal samples in our affected cats did not reveal the presence of melanin, unlike a previous report documenting the presence of melanin particles in feline corneal sequestra.[8] Many of the larger circular to irregularly shaped, electron-dense deposits scattered over and amidst necrotic collagen fibrils in one of the affected tissues appeared compatible with mineralization. A mineralized corneal sequestrum has been previously reported in a cat.[2] The proposed pathophysiologic mechanism of mineralization in the case involved FHV-1 infection, and stromal inflammation and necrosis with release of collagenolytic enzymes that contributed to an environment conducive to calcium-phosphate precipitation.[2] One previous case report has documented the presence of iron (Fe) in a corneal sequestrum from a cat.[10] A more recent study assessing the elemental peaks in feline corneal sequestra reported the presence of Fe, copper and small amounts of transient metals, among other elemental components.[8] The ultrastructural appearance of some of these smaller, more electron-dense deposits in the current cases may be consistent with Fe or other metallic deposits.

Similar to previously reported TEM findings from a feline corneal sequestrum,[4] large numbers of coccoid bodies were noted in one affected cornea in our study (case 2; Table 1). The coccoid-like organisms detected in the corneal lesion in case 2 had ultrastructural features compatible with *Staphylo-*

coccus sp. This bacterium was probably a secondary invader. Various secondary invaders have been isolated from corneal sequestra including *Staphylococcus* sp.[1,4,11] In the present study, *Chlamydophila felis* and *Mycoplasma* spp. inclusions were not detected in the corneal sequestra by either HR-LM or TEM. The DNA of either of these organisms was not found in the corneal samples or blood of the cases assessed by PCR. A previous study documented 30 of 31 cats with corneal sequestration, using indirect immunofluorescent antibody assays performed on conjunctival scrapings, as negative for *Chlamydia psittaci*.[3] Our results, using PCR and TEM on a portion of the corneal sequestrum, provide further support that *Chlamydophila felis* is probably not a major primary pathogen or secondary invader in cats with corneal sequestration.

TEM is considered to be the gold standard for detecting apoptotic cells.[12] In the present study, all corneal sequestra, independent of the presence of DNA of the infectious agents assessed, exhibited occasional keratocytes with morphology indicative of apoptosis including clumping and margination of chromatin, and shrunken cytoplasm. One corneal sequestrum also exhibited apoptotic epithelial cells. Apoptosis is a form of involutional programmed cell death with limited inflammation or little release of cellular contents, including enzymes that could cause degradation of adjacent tissues and cells.[13] Minimization of collateral damage to sensitive ocular tissues by a process such as apoptosis may be important.[14] Specifically, apoptosis has been reported in the early development of ocular viral infections[15] and is thought to be an important mechanism for protection against viral infection in the eye.[16] In particular, herpes simplex virus (HSV)-1 infection of corneal epithelium of rabbits has been reported to cause anterior stromal keratocyte apoptosis underlying the site of epithelial injury.[15] These authors hypothesized that soluble mediators released by the HSV-1 epithelial injury mediated anterior keratocyte apoptosis and that the epithelial-stromal apoptotic system evolved, in part, to limit viral extension to the deeper layers of the cornea.[15] It is also speculated that apoptosis of keratocytes and epithelial cells following keratitis prevents further corneal stromal damage caused, not only by pathogens, but also by migrating inflammatory cells.[15,17] The apoptotic keratocytes noted using TEM on the corneal tissues from affected cats in our study may serve to limit corneal extension of FHV-1, and to prevent further stromal damage as a result of the peri- and intralesional neutrophils and mononuclear cells.

An important link between apoptosis of ocular tissues and the pathogenesis of ocular toxoplasmosis has been previously proposed by Hu *et al*.[16] In experimentally induced *T. gondii* corneal disease in mice, apoptotic changes were seen in cells in the cornea, in particular the epithelium at day 1 and 2 and stromal keratocytes at day 4, following intracameral inoculation of the eyes with *T. gondii* tachyzoites.[16] In that study, the authors were unable to determine whether the apoptosis of ocular tissues was evoked directly by the parasite or indirectly through the inflammatory cells which had interacted with the parasites.[16] Regardless, apoptosis of

corneal epithelial cells and keratocytes, whether *T. gondii* or FHV-1-associated or not, is likely to be important in the pathogenesis of feline corneal sequestration.

Despite the positive PCR results for *T. gondii* (*n* = 4 cases) and FHV-1 (*n* = 2 cases) in the corneal sequestra samples in our study, presence of either of these organisms could not be obtained by either HR-LM or TEM. Hu *et al.* 2001 reported that apoptotic inflammatory cells disappeared from murine eyes by day 4 following *T. gondii* inoculation. This finding led them to speculate that some ocular cells may digest the parasites from these apoptotic inflammatory cells.[16] In the current study, TEM revealed macrophages phagocytizing in the corneal sequestra. It is possible that the inflammatory cells in the corneal sequestra digested the organisms from the apoptotic keratocytes thereby leaving their remnants, which were detectable with PCR. Polymerase chain reaction is a very sensitive test in that it is used to amplify specific portions of microbial DNA, which allows detection of minuscule amounts of target DNA in specimens.[18]

To our knowledge, DNA from *T. gondii* has not been previously found in naturally occurring corneal disease, including feline corneal sequestration. Toxoplasmosis, caused by *Toxoplasma gondii*, an obligate intracellular protozoal parasite, is one of the most common parasitic infections of animals worldwide.[19] The means by which toxoplasmosis is mainly spread are: (1) transplacental transmission, (2) ingestion of infected tissues, and (3) ingestion of food or water contaminated with infective feces.[19] The indoor/outdoor status of two of the *T. gondii* DNA-positive cats (cases 1 and 8; Table 1) in this study could have provided a means of exposure of these cats to the parasite.

Classic ocular abnormalities reported with toxoplasmosis in cats include multifocal to diffuse chorioretinitis, retinochoroiditis, anterior uveitis, and optic neuritis. Most recent studies of feline ocular toxoplasmosis, both clinical and experimental in nature, have documented that the posterior segment is most commonly affected with the choroid being altered primarily, and retinitis resulting secondarily.[20–22] Chorioretinitis is the most common ocular lesion caused by *T. gondii* in cats.[23]

Toxoplasma gondii DNA was detected with PCR in four of the nine corneal sequestra and was also positive in the blood of two of these four affected cats. PCR for amplification of *T. gondii* DNA from other biologic specimens, including aqueous humor of humans and cats, has previously been reported.[24–28] One report documented the detection of *T. gondii* within the aqueous humor of cats using PCR following oral inoculation with *T. gondii* tissue cysts.[29] A clinical study revealed that 2 of 23 (8.7%) healthy cats and 8 of 43 (18.6%) cats with uveitis had *T. gondii* detected in aqueous humor by PCR, indicating that the presence of this organism may correlate to clinical disease in some cats.[24] Similar findings have been reported regarding FHV-1 detection by PCR in the aqueous humor of both healthy cats and cats with uveitis,[30] and in corneas of both healthy cats and cats with corneal sequestra.[31,32] In the current study, the presence

of *T. gondii* DNA in the corneal sequestra and in the blood of two cases (cases 1 and 2; Table 1) and positive IgG titers in the two other cats from which *T. gondii* DNA was isolated from the corneal sequestra (cases 6 and 8; Table 1) suggests that *T. gondii* may have played a role in the pathogenesis of corneal sequestration in these cats. However, as *T. gondii* DNA and antigens have previously been detected in body fluids, including aqueous humor and serum, of healthy and ill cats,[24,29,33–35] our positive PCR results do not support a definitive causal association between *T. gondii* and feline corneal sequestra. FHV-1 DNA was also detected in the blood of three of these four *T. gondii*-positive cases and in the affected corneal tissue of one such cat. FHV-1 may have contributed to the development of the corneal sequestra in these cases.

It is likely that *T. gondii* gained access to these feline corneas hematogenously as two of four cats with the presence of *T. gondii* DNA detected in the keratectomy specimens were positive for *T. gondii* DNA in the blood, and had corneal vascularization clinically. However, one of four cats positive for *T. gondii* DNA in the corneal sequestrum and having a positive IgG titer against *T. gondii* did not have corneal vascularization or *T. gondii* DNA detected in the blood. This suggests that *T. gondii* may have gained access to the cornea hematogenously during an earlier active phase of infection or by an alternate route. Toxoplasmosis has been documented to cause corneal lesions in mice following experimental intracameral injection of *T. gondii* tachyzoites.[16] This finding, in addition to the documentation of *T. gondii* DNA in the aqueous humor of cats with and without uveitis, suggest that *T. gondii* organisms may have the opportunity to affect the feline cornea through their presence in the aqueous humor. Unfortunately, given the retrospective nature of this clinical study and the classic presenting features of corneal sequestration in these cats, the status of the aqueous humor in these animals was not assessed. As such, the exact mode by which *T. gondii* gained access to these feline corneas and whether or not it is a secondary invader or primary pathogen in feline corneal sequestration remain unknown.

Apoptosis may play a role in the pathogenesis of feline corneal sequestration independent of the presence of DNA of these infectious organisms. Prospective clinical studies are warranted to further understand the significance, if any, of *T. gondii* in relation to feline corneal sequestration.

ACKNOWLEDGMENTS

REFERENCES

1. Gelatt KN, Peiffer L, Stevens J. Chronic ulcerative keratitis and sequestrum in the domestic cat. *Journal of the American Animal Hospital Association* 1973; **9**: 204–213.

2. Gemensky AJ, Wilkie DA. Mineralized corneal sequestrum in a cat. *Journal of the American Veterinary Medical Association* 2001; **219**: 1568–72, 1550.

3. Morgan RV. Feline corneal sequestration: a retrospective study of 42 cases (1987–1991). *Journal of the American Animal Hospital Association* 1994; **30**: 24–28.

4. Souri E. The feline corneal nigrum. *Veterinary Medicine/Small Animal Clinician* 1975; **70**: 531–534.

5. Startup FG. Corneal necrosis and sequestration in the cat: a review and record of 100 cases. *Journal of Small Animal Practice* 1988; **29**: 476–486.

6. Hakanson NE, Dubielzig RR. Chronic superficial corneal erosions with anterior stromal sequestration in three horses. *Veterinary and Comparative Ophthalmology* 1994; **4**: 179–183.

7. Cullen CL, Njaa BL, Grahn BH. Ulcerative keratitis associated with qualitative tear film abnormalities in cats. *Veterinary Ophthalmology* 1999; **2**: 197–204.

8. Featherstone HJ, Franklin VJ, Sansom J. Feline corneal sequestrum: laboratory analysis of ocular samples from 12 cats. *Veterinary Ophthalmology* 2004; **7**: 229–238.

9. Matsubara M, Zieske JD, Fini ME. Mechanism of basement membrane dissolution preceding corneal ulceration. *Investigative Ophthalmology and Visual Science* 1991; **32**: 3221–3237.

10. Ejima H, Hara N, Kajigaya H. Detection of iron in a blackish lesion in a case of feline corneal sequestration. *Journal of Veterinary Medical Science* 1993; **55**: 1051–1052.

11. Gelatt KN. Corneal sequestration in a cat. *Veterinary Medicine/Small Animal Clinician* 1971; **66**: 561–562.

12. Yasuhara S, Zhu Y, Matsui T *et al*. Comparison of comet assay, electron microscopy, and flow cytometry for detection of apoptosis. *Journal of Histochemistry and Cytochemistry* 2003; **51**: 873–885.

13. Depraetere V, Golstein P. Fas and other cell death signaling pathways. *Seminars in Immunology* 1997; **9**: 93–107.

14. Mohan RR, Liang Q, Kim WJ *et al*. Apoptosis in the cornea: further characterization of Fas/Fas ligand system. *Experimental Eye Research* 1997; **65**: 575–589.

15. Wilson SE, Pedroza L, Beuerman R *et al*. Herpes simplex virus type-1 infection of corneal epithelial cells induces apoptosis of the underlying keratocytes. *Experimental Eye Research* 1997; **64**: 775–779.

16. Hu S, Schwartzman JD, Kasper LH. Apoptosis within mouse eye induced by *Toxoplasma gondii*. *Chinese Medical Journal* 2001; **114**: 640–644.

17. Podskochy A, Fagerholm P. The expression of Fas ligand protein in ultraviolet-exposed rabbit corneas. *Cornea* 2002; **21**: 91–94.

18. Belak S, Ballagi-Pordany A. Application of the polymerase chain reaction (PCR) in veterinary diagnostic virology. *Veterinary Research Communications* 1993; **17**: 55–72.

19. Dubey JP. Toxoplasmosis. *Veterinary Clinics of North America: Small Animal Practice* 1987; **17**: 1389–1404.

20. Chavkin MJ, Lappin MR, Powell CC *et al*. Seroepidemiologic and clinical observations of 93 cases of uveitis in cats. *Progress in Veterinary and Comparative Ophthalmology* 1992; **2**: 29–36.

21. Davidson MG, Lappin MR, English RV *et al*. A feline model of ocular toxoplasmosis. *Investigative Ophthalmology and Visual Science* 1993; **34**: 3653–3660.

22. Dubey JP, Carpenter JL. Histologically confirmed clinical toxoplasmosis in cats: 100 cases (1952–1990). *Journal of the American Veterinary Medical Association* 1993; **203**: 1556–1566.

23. Davidson MG, English RV. Feline ocular toxoplasmosis. *Veterinary Ophthalmology* 1998; **1**: 71–80.

24. Lappin MR, Burney DP, Dow SW *et al*. Polymerase chain reaction for the detection of *Toxoplasma gondii* in aqueous humor of cats. *American Journal of Veterinary Research* 1996; **57**: 1589–1593.

25. Stiles J, Prade R, Greene C. Detection of *Toxoplasma gondii* in feline and canine biological samples by use of the polymerase chain reaction. *American Journal of Veterinary Research* 1996; **57**: 264–267.

26. Aouizerate F, Cazenave J, Poirier L *et al*. Detection of *Toxoplasma gondii* in aqueous humour by the polymerase chain reaction. *British Journal of Ophthalmology* 1993; **77**: 107–109.

27. Chan CC, Palestine AG, Li Q *et al*. Diagnosis of ocular toxoplasmosis by the use of immunocytology and the polymerase chain reaction. *American Journal of Ophthalmology* 1994; **117**: 803–805.

28. Jones CD, Okhravi N, Adamson P *et al*. Comparison of PCR detection methods for B1, P30, and 18S rDNA genes of *T. gondii* in aqueous humor. *Investigative Ophthalmology and Visual Science* 2000; **41**: 634–644.

29. Burney DP, Chavkin MJ, Dow SW *et al*. Polymerase chain reaction for the detection of *Toxoplasma gondii* within aqueous humor of experimentally-inoculated cats. *Veterinary Parasitology* 1998; **79**: 181–186.

30. Maggs DJ, Lappin MR, Nasisse MP. Detection of feline herpesvirus-specific antibodies and DNA in aqueous humor from cats with or without uveitis. *American Journal of Veterinary Research* 1999; **60**: 932–936.

31. Stiles J, McDermott M, Bigsby D *et al*. Use of nested polymerase chain reaction to identify feline herpesvirus in ocular tissue from clinically normal cats and cats with corneal sequestra or conjunctivitis. *American Journal of Veterinary Research* 1997; **58**: 338–342.

32. Nasisse MP, Glover TL, Moore CP *et al*. Detection of feline herpesvirus 1 DNA in corneas of cats with eosinophilic keratitis or corneal sequestration. *American Journal of Veterinary Research* 1998; **59**: 856–858.

33. Burney DP, Lappin MR, Spilker M *et al*. Detection of *Toxoplasma gondii* parasitemia in experimentally inoculated cats. *Journal of Parasitology* 1999; **85**: 947–951.

34. Lappin MR, Greene CE, Prestwood AK *et al*. Enzyme-linked immunosorbent assay for the detection of circulating antigens of *Toxoplasma gondii* in the serum of cats. *American Journal of Veterinary Research* 1989; **50**: 1586–1590.

35. Lappin MR, Cayatte S, Powell CC *et al*. Detection of *Toxoplasma gondii* antigen-containing immune complexes in the serum of cats. *American Journal of Veterinary Research* 1993; **54**: 415–419.